Optics Letters

# Tunable radio frequency photonics filter using a comb-based optical tapped delay line with an optical nonlinear multiplexer

Morteza Ziyadi,[1,*] Amirhossein Mohajerin-Ariaei,[1] Mohammad Reza Chitgarha,[1] Salman Khaleghi,[1] Ahmed Almaiman,[1] Yinwen Cao,[1] Amin Abouzaid,[2] Bishara Shamee,[1] Moshe Tur,[3] Loukas Paraschis,[4] Carsten Langrock,[5] Martin M. Fejer,[5] Joseph D. Touch,[2] and Alan E. Willner[1]

[1]Department of Electrical Engineering, University of Southern California, Los Angeles, California 90089, USA
[2]Information Sciences Institute, University of Southern California, 4676 Admiralty Way, Marina del Rey, California 90292, USA
[3]School of Electrical Engineering, Tel Aviv University, Ramat Aviv 69978, Israel
[4]Cisco Systems, 170 W. Tasman Drive, San Jose, California 95134, USA
[5]Edward L. Ginzton Laboratory, Stanford University, Stanford, California 94305, USA
*Corresponding author: ziyadi@usc.edu

Received 20 April 2015; revised 12 June 2015; accepted 13 June 2015; posted 15 June 2015 (Doc. ID 238360); published 6 July 2015

**A radio frequency (RF) photonic filter is experimentally demonstrated using an optical tapped delay line (TDL) based on an optical frequency comb and a periodically poled lithium niobate (PPLN) waveguide as multiplexer. The approach is used to implement RF filters with variable bandwidth, shape, and center-frequency.** 

***OCIS codes:*** (060.2360) Fiber optics links and subsystems; (060.4370) Nonlinear optics, fibers.

http://dx.doi.org/10.1364/OL.40.003284

Radio frequency (RF) and microwave photonics have many applications due to their low loss and high bandwidth. Their uses generally require accurate signal filtering and processing [1–3]. These filters are more useful when they can be dynamically reconfigured by tuning their bandwidth, shape, and center frequency using optical signal processing methods [4,5].

Several tunable RF photonic filters have been demonstrated. In one approach, optical filters based on fiber Bragg gratings or stimulated Brillouin scattering are used to filter the RF sidebands [6,7]. In several other approaches, a tapped delay line (TDL) structure is used as a key building block to create complex RF photonic filters [8–13]. In the TDL approach, the RF signal is copied into $N$ optical taps that are weighted by coefficients, after which the taps are multiplexed and detected by a photodiode. This structure employs finite impulse response (FIR) filters in the frequency domain. Previous reports have demonstrated tunable tap-based RF filters whose complex tap coefficients can be varied [8–13]. These designs multiplex the tapped signals in the electrical domain, following the photodetectors [8–13]. Although these approaches produce tunable RF filter functions, they do not easily permit further optical signal processing or transmission, since they involve optoelectronic detection.

In this Letter, we experimentally demonstrate a variable bandwidth, shape, and center-frequency RF photonic filter using a continuously tunable comb-based optical tapped delay line (OTDL) with a single optical nonlinear multiplexer and an optical output [14–16]. In [16], we used a comb-based OTDL to implement Nyquist filters in the optical domain to generate Nyquist signals. In this Letter, we use a similar approach to implement the FIR filters for the application of RF and microwave photonics. Moreover, in this work, the tunability and reconfigurability of the approach are studied and experimentally shown. In this approach, the input RF signal is modulated on the frequency lines of an optical frequency comb to create the taps of the OTDL, which are delayed by a dispersive element. A periodically poled lithium niobate (PPLN) crystal nonlinearly multiplexes the TDLs in the optical domain to achieve the optical filter output, which then can be used for further optical processes. An electrical filter output can be derived using a photodiode. The demonstration includes tunable complex coefficient RF filters with different bandwidths of $<1$ GHz, as well as of 8 and 32 GHz, and tunability over the center frequency and different shapes, e.g., Sinc and Gaussian.

The concept of an RF-FIR filter using a TDL structure is shown in Fig. 1. The input signal is copied onto $N$ paths and each path is delayed and multiplied by an appropriately complex weight. The weighted, delayed taps are summed in the time domain, and FIR filtering is implemented in the frequency domain. Figure 2 depicts an RF photonic filter using a frequency comb-based OTDL. The optical TDL structure requires coherent multiplexing, which is achieved by using a mode-locked laser to generate the coherent pump components. A programmable phase/amplitude filter, such as a spatial light

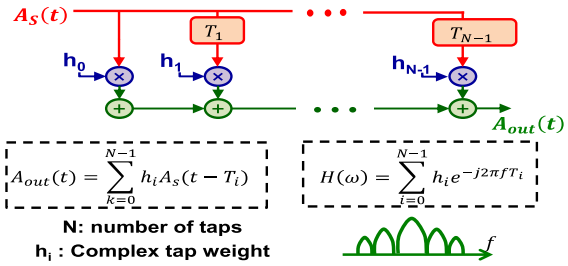


**Fig. 1.** Concept of the FIR filter using a TDL structure.

modulator filter based on liquid crystal-on-silicon (LCoS) technology, separates the frequency lines of the comb source into two paths: the dummy pumps ($A_D$) and the signals ($A_S$). The number of frequency components on each path is equal to the number of taps, i.e., $N$, in the FIR filter. The frequency comb lines of the signal path are modulated with the RF signal, $A_S(t)$, which is generated by a vector network analyzer (VNA). The result generates $N$ coherent copies of the RF signal on the comb lines. These replicas are sent through a frequency-dependent optical delay element [such as a dispersion compensating fiber (DCF)] to induce signal delays with a relative delay of $\Delta\tau = D \times \Delta\lambda$, where $D$ is the dispersion parameter (picosecond/nanometer) and $\Delta\lambda$ is the wavelength separation (nanometers) between two adjacent frequency lines. Thus, $T_i$ in the FIR becomes $T_i = i \cdot \Delta\tau$, $i = 0, 1, \ldots, (N-1)$. Other RF filters with different bandwidths can be achieved by changing the delay, which this architecture supports by changing the pump-frequency spacing in the comb source or by varying the length of the DCF. The frequency lines of the dummy pumps are sent through the same DCF to increase stability. The delayed signals ($A_{S,i} = A_S(t - i \cdot \Delta\tau)$, $i = 0, 1, \ldots, (N-1)$) are equivalent to the OTDL taps that are coherently combined with the dummy pumps and act as tap weights. A PPLN waveguide with a quasi-phase matching (QPM) frequency of $f_{\mathrm{QPM}}$ multiplexes the taps with the dummy pumps. The tap weights are tuned using a programmable filter to introduce arbitrary phase and amplitude, $A_{F,i}$, on the frequency lines. Inside the PPLN waveguide, in a sum-frequency generation process, each replica of the signal $A_{S,i}$ at frequency $f_{S,i}$ combines with a pump $A_{D,i}$, which is chosen from the dummy pumps group at frequency $f_{D,i} = 2f_{\mathrm{QPM}} - f_{S,i}$ to generate a new signal at a frequency of $f_{D,i} + f_{S,i} = 2f_{\mathrm{QPM}}$ with a value proportional to $A_{S,i} \cdot A_{D,i} \cdot A_{F,i}$, $i = 0, 1, \ldots, (N-1)$. Because all signal replicas and dummy pumps are mutually coherent, the resulting signal at $2f_{\mathrm{QPM}}$ is the coherent sum of all of the signals at that frequency, i.e., the signal $\sum_i (A_{S,i}.A_{D,i}.A_{F,i})$ is generated at $2f_{\mathrm{QPM}}$. However, because the signal and pumps wavelengths are in the C band, i.e., around 1550 nm, the generated signal will have a wavelength near 750 nm, which cannot propagate in the optical fiber. To convert the generated signal at the second harmonic back to the C band, another pump laser, $A_P$, which is located at $f_{\mathrm{pump}}$ is injected into the PPLN waveguide using the difference-frequency generation process. Thus, the output of the process at $f_{\mathrm{out}} = 2f_{\mathrm{QPM}} - f_{\mathrm{pump}}$ is

$$A_{\mathrm{out}}(t) \propto \sum_{i=0}^{N-1} A_P^* \cdot A_{D,i} \cdot A_{F,i} \cdot A_S(t - i\Delta\tau), \tag{1}$$

in which $A_P^*$ is the complex conjugate of the electrical field of the pump. Assuming, $h_i = A_P^* \cdot A_{D,i} \cdot A_{F,i}$, the output becomes

$$A_{\mathrm{out}}(t) \propto \sum_{i=0}^{N-1} h_i A_S(t - i\Delta\tau), \tag{2}$$

which is the FIR filter equation. The resulting FIR filter is a periodic filter with a free spectral range (FSR) of $1/\Delta\tau$, which can be tuned by varying the relative delay. The desired filtering at the output could be achieved by adjusting the phase and amplitude of the coherent pumps to the tap weights of the FIR filter. The output of the designed FIR filter can be either (a) kept in the optical domain or (b) transferred to the RF domain using a photodiode, whose electrical output can be analyzed in the VNA. Keeping the signal in the optical domain further enables the optical processing of the RF signal.

Figure 3 shows the experimental setup for the RF photonic filter using a comb-based OTDL. A mode-locked laser with a 10 GHz repetition rate and 2 ps pulse width generates a coherent frequency comb, which passes through a delay line interferometer with an FSR of 20 GHz to increase its frequency spacing. The resulting 20 GHz frequency comb is sent through an erbium-doped fiber amplifier (EDFA) and a highly

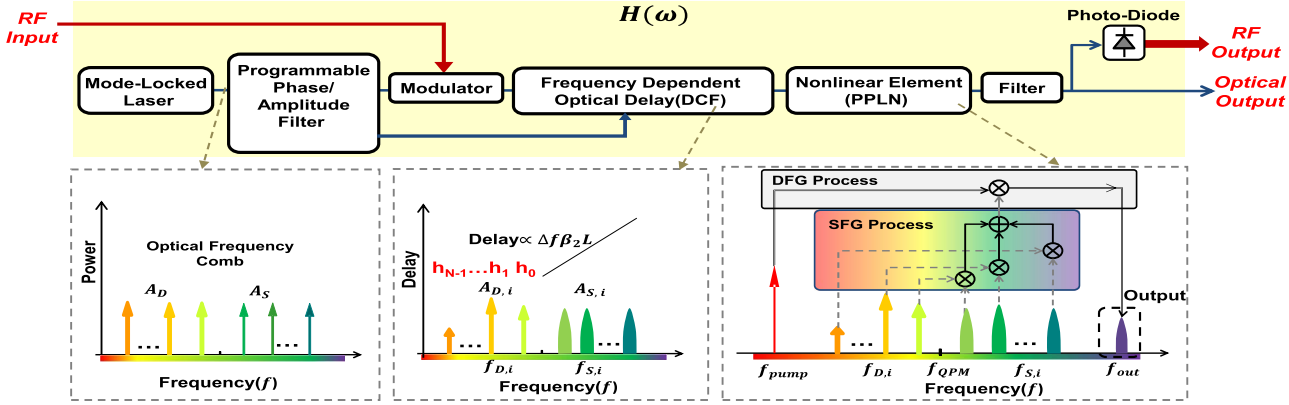


**Fig. 2.** Concept of the RF photonic FIR filter using a comb-based OTDL, in which the optical comb provides the taps of the FIR filter. This concept also utilizes a DCF to delay the tapped RF-modulated signals and to multiplex them in a PPLN.

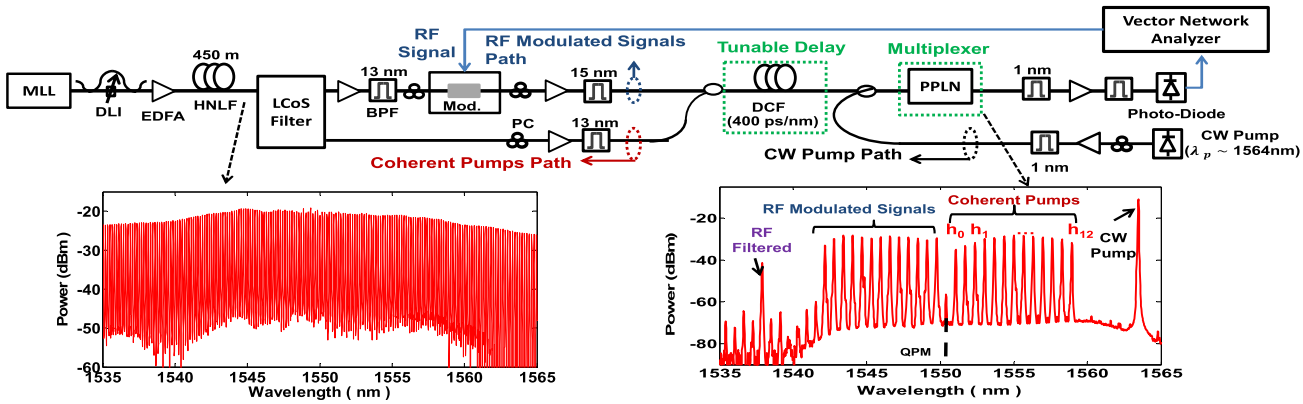


**Fig. 3.** Experimental setup and optical spectrum of the signals for the RF photonic FIR filter using a comb-based OTDL. BPF, bandpass filter; PC, polarization controller.

nonlinear fiber to generate a flat and broad spectrum (as shown in the figure). A programmable phase and amplitude filter based on LCoS technology is used to select and write complex weights on the frequency comb lines, and to separate the lines into two paths: the signals and the coherent pumps. For each path, up to 13 comb lines are selected with a frequency spacing of 80 GHz (0.64 nm). After pre-amplification in an intensity modulator, an RF signal is generated along the signal path by a VNA, and is modulated on the frequency lines. After sufficient EDFA amplification, the signals and pumps travel through a DCF to introduce relative delays on the signals that act as a delay line in the FIR filter. With another amplified continuous-wave laser pump at ~1564 nm, all the signals and pumps are sent into a 4-cm-long PPLN waveguide with a temperature-tuned QPM wavelength of ~1550.5 nm, which is the middle point of the selected comb lines. This creates the photonic RF-FIR filter with the optical spectrum shown in the figure. It should be mentioned that the rate of change in the phase matching of the PPLN waveguide is 0.13 nm/°C and in our experiment, the variations of ±0.5°C do not have too much effect. However, high QPM detuning would cause less conversion efficiency, corresponding to the lower performance of the system. The output signal is filtered and sent to a photodiode to be analyzed in the VNA.

The tap weights, $h_i$s, must be calibrated to tune the RF filter properties, such as shape, bandwidth, etc. The calibration process is similar to the approach presented in [16]. The tap weights are calibrated to the appropriate values, with the central tap selected as the reference tap. In order to calibrate the tap-$k$ coefficient, the coefficients are set as $h_i = 1$ for the reference tap and tap-$k$ and $h_i = 0$ for the rest of the taps. The corresponding pump is disabled to set the coefficient to 0. To tune the coefficient to 1, the amplitude and phase of the corresponding pump are tuned in the LCoS filter to achieve a symmetric shape at the output spectrum. In fact, complex coefficients are tuned by the LCoS filter to implement the calibration process. After calibrating all the taps, the amplitude and phase of the taps are adjusted to the tap weights of the desired FIR filter.

Figures 4(a)–4(c) show the experimental and simulated results using a DCF with dispersion parameter of 80 ps/nm, which generates an FIR filter with an FSR of ~20 GHz. Nine frequency lines implement a nine-tap FIR filter in which the amplitude and phase of the taps is tuned to achieve different shapes and bandwidths (BWs). The experimental result is similar to the simulated design. Filters with BWs of <1 GHz and ~3 GHz can be implemented. Moreover, different ratios of the main lobe to the side lobe of 10–20 dB are measured. This approach is the same as a TDL implementation in the RF domain using optical waves. Thus, after calibration, the tap coefficients are the same as in the simulation, which facilitates the tuning of the filter properties. The FSR of the filter can be tuned to 12 GHz by replacing the DCF with one that supports ~130 ps/nm, the result of which is shown in Fig. 4(d). Using a ~400 ps/nm DCF, we can achieve a filter with an FSR of

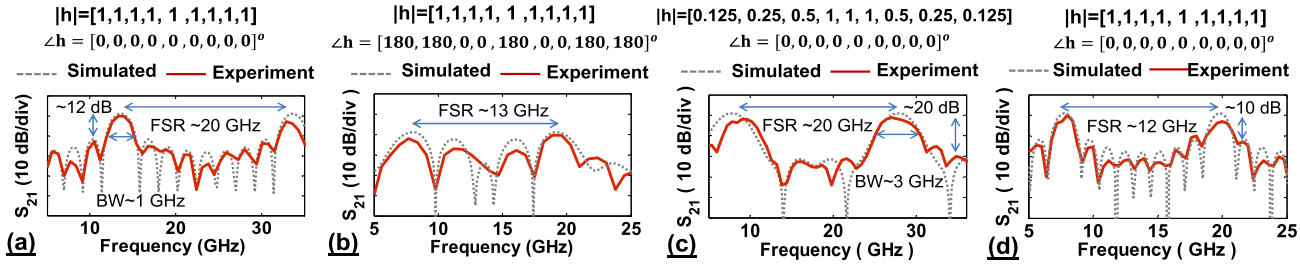


**Fig. 4.** Experimental results for 9-tap RF-FIR photonic filters with (a)–(c) showing an FSR of 20 GHz using an 80 ps/nm DCF. The tap coefficients ($h$) are tuned in both phase and amplitude to implement different filters. (d) An FSR of 12 GHz using 130 ps/nm DCF. Experimental results match the simulated design.

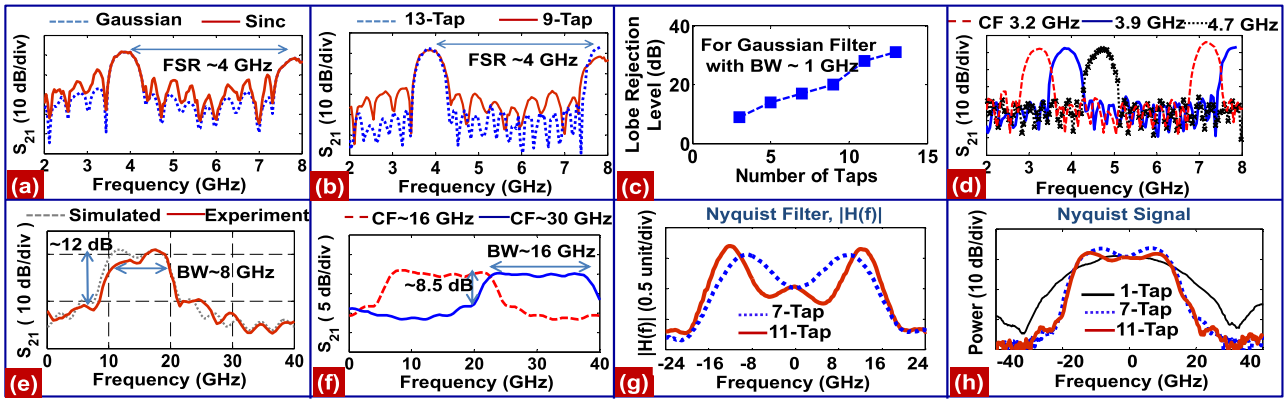


**Fig. 5.** Experimental results: (a) different shapes for a 9-tap FIR filter with an FSR of 4 GHz using a 400 ps/nm DCF. (b) Tunability over the number of taps. (c) Measured lobe rejection level for the filters of part (b). (d) Tunability over the central frequency. (e) An FIR filter with a BW of 8 GHz using a 40 ps/nm DCF. (f) A tunable FIR filter with a BW of 16 GHz. (g) Nyquist filter with a BW of 32 GHz. (h) Generated optical Nyquist signal.

4 GHz, as shown in Figs. 5(a)–5(d). RF filters with different number of taps and shapes can also be implemented [see Figs. 5(a) and 5(b)]. For the sinc(sinc($x$) = sin($x$)/$x$) shape, the taps all have the same coefficient. As shown in Fig. 5(c), increasing the number of taps achieves filters with a high value of lobe rejection level measured as a ratio of the main lobe to the side lobes. Achieving filters with different shapes and bandwidth and lobe rejection levels shows the reconfigurability of the approach.

The ability to implement complex coefficients allows us to tune the center frequency (CF) of the filter, as shown in Fig. 5(d). The slight variation of the phase on the tap coefficients, which is equivalent to the frequency shift, is utilized to tune the CF of the filter [15]. This could be implemented by choosing complex tap coefficients in the LCoS filter. For instance, in Fig. 5(d), the taps of the filter at the CF of 3.9 GHz have phase values of [0,–60,–120,170,100,45, –20,–80,–140,150,90] deg compared to the filter at the CF of 3.2 GHz.

This approach can also implement very broad band filters. To achieve a broad band filter with the range of several gigahertz, the tap delay time is changed by varying either the wavelength spacing of the frequency comb lines or the length of the DCF. Figure 5(e) illustrates how use of a 40 ps/nm DCF can implement a filter with an FSR of 40 GHz and a bandwidth of ~8 GHz. By reconfiguring the tap coefficients, filters with the BW of 16 GHz and different CFs are implemented [see Fig. 5(f)]. Frequency lines with a spacing of 120 GHz (0.965 nm) and a 16 ps/nm DCF can implement Nyquist filters with the BW of 32 GHz to generate optical Nyquist data channels at 32 Gbaud [see Figs. 5(g) and 5(h)]. The tunability of these broad band filters is demonstrated by implementing Nyquist filters at a 26 GHz bandwidth, as shown in [16]. In conclusion, RF-FIR photonic filters can be generated with complex coefficients. Tunable FIR filters with a wide range of parameters can be achieved using a comb-based OTDL in a single PPLN waveguide. Implementing the FIR filter in the time domain using an OTDL enables further optical processing of the filtered RF signal.

**Funding.** Center for Integrated Access Network (CIAN); National Science Foundation (NSF).

## REFERENCES

1. J. Capmany, B. Ortega, and D. Pastor, J. Lightwave Technol. **24**, 201 (2006).
2. R. A. Minasian, IEEE Trans. Microwave Theory Tech. **54**, 832 (2006).
3. A. J. Seeds and K. J. Williams, J. Lightwave Technol. **24**, 4628 (2006).
4. J. Yao, J. Lightwave Technol. **27**, 314 (2009).
5. J. Capmany, J. Mora, I. Gasulla, and J. Sancho, J. Lightwave Technol. **31**, 571 (2013).
6. J. Palaći, P. Perez-Millan, G. E. Villanueva, J. L. Cruz, M. V. Andŕes, J. Marti, and B. Vidal, IEEE Photon. Technol. Lett. **22**, 1467 (2010).
7. W. Zhang and R. A. Minasian, IEEE Photon. Technol. Lett. **23**, 1775 (2011).
8. V. R. Supradeepa, C. M. Long, R. Wu, F. Ferdous, E. Hamidi, D. E. Leaird, and A. M. Weiner, Nat. Photonics **6**, 186 (2012).
9. X. Xue, X. Zheng, H. Zhang, and B. Zhou, J. Lightwave Technol. **31**, 2263 (2013).
10. L. Li, X. Yi, T. X. H. Huang, and R. A. Minasian, Opt. Express **20**, 11517 (2012).
11. A. Ortigosa-Blanch, J. Mora, J. Capmany, B. Ortega, and D. Pastor, Opt. Lett. **31**, 709 (2006).
12. X. Xue, Y. Xuan, H.-J. Kim, J. Wang, D. E. Leaird, M. Qi, and A. M. Weiner, J. Lightwave Technol. **32**, 3557 (2014).
13. H.-J. Kim, D. E. Leaird, A. J. Metcalf, and A. M. Weiner, J. Lightwave Technol. **32**, 3478 (2014).
14. M. Ziyadi, M. R. Chitgarha, S. Khaleghi, A. Mohajerin-Ariaei, A. Almaiman, J. Touch, M. Tur, C. Langrock, M. M. Fejer, and A. E. Willner, Opt. Express **22**, 84 (2014).
15. M. Ziyadi, A. Mohajerin-Ariaei, M. Chitgarha, S. Khaleghi, A. Almaiman, A. Abouzaid, J. Touch, M. Tur, L. Paraschis, C. Langrock, M. M. Fejer, and A. Willner, "Experimental demonstration of a variable bandwidth, shape and center-frequency RF photonics filter using a continuously tunable optical tapped-delay-line and having an optical output," in *CLEO: 2014, OSA Technical Digest* (online) (Optical Society of America, 2014), paper STu3I.4.
16. M. Ziyadi, M. R. Chitgarha, A. Mohajerin Ariaei, S. Khaleghi, A. Almaiman, Y. Cao, M. J. Willner, M. Tur, L. Paraschis, C. Langrock, M. M. Fejer, J. D. Touch, and A. E. Willner, Opt. Lett. **39**, 6585 (2014).